# Acoustic Transmissions for Wireless Communications and Power Supply in Biomedical Devices

## Graham Wild and Steven Hinckley

School of Engineering, Edith Cowan University, 270 Joondalup Drive, Joondalup WA 6027, Australia

**PACS:** 43.80.Vj, 84.40.Ua, 84.30.Jc

## ABSTRACT

In this paper, we demonstrate the principle of acoustic transmission for communications and power supply, in-vivo. The acoustic transmissions are intended to be used for fixed implanted biomedical devices, such as pacemakers, but more importantly, neural implants were wired and wireless RF communications cannot be used. The acoustic transmissions can be used for both wireless communications and to recharge the device, in-vivo, using conventional piezoelectric power harvesting techniques. Current research in biomedical engineering is looking at implantable devices to regulate conditions such as Parkinson's and other neuromuscular conditions. Transient devices, such as those used in the gastrointestinal track, make use of high frequency RF, were the permittivity of the human body begins to decrease. However, significant power is still required. This results in local tissue heating, due to the absorption of the EM radiation. This heating has side effects that limit the exposure times for safe practices. For neural implants, were the goal is to have the product implanted for long periods of time, without complications and minimal side effects, RF communications cannot currently be used. Acoustic transmissions represent an ideal low power method of communicating with in-vivo biomedical devices, and for recharging them through power harvesting. In this work, we present results showing the performance of the communications channel and sample communications signals, through a biological specimen. The frequency response, transfer function and transient response (at resonance) of the communications channel were measured. Due to the frequency response of the communications channel, PSK was chosen as the modulation method. Successful communication was achieved through the communications channel. We also show the result of preliminary work on harvesting the acoustic signals to provide power for recharging in-vivo Biomedical devices.

## INTRODUCTION

Current biomedical engineering research is looking at implantable devices to regulate conditions such as Parkinson's and other neuromuscular conditions [1]. Transient devices, such as those used in the gastrointestinal track, make use of high frequency RF, were the permittivity of the human body begins to decrease [2]. However, significant power is still required for communications. This results in local tissue heating due to the absorption of the EM radiation. This heating has side effects that limit the exposure times for safe practices [3-5]. For neural implants, were the goal is to have the product implanted for long periods of time, without complications and minimal side effects, RF communications is not currently used.

Wireless acoustic communications represents an ideal, low power method of communicating with in-vivo biomedical devices. Acoustic communications has previously been proposed for communications in Structural Health Monitoring (SHM) systems, were autonomous robotic agents are used for inspection and repair [6-8]. Here, acoustic signals were successfully shown to be used for transmitting relatively high data rates (up to 100kbps) using piezoelectric transducers and aluminium panelling.

The added advantage of utilising acoustic communications is the use of a piezoelectric receiver. This means that current work into piezoelectric power harvesting [9] could be utilised for supplying power to the in-vivo biomedical devices. The same acoustic transmission used to communicate can in fact be used for power harvesting.

In this paper, we use acoustic transmissions to both communicate wirelessly, and supply power to in-vivo biomedical devices. The acoustic transmissions channel is made up of several layers. These include;

- a piezoelectric transducer as the transmitter,
- a coupling medium,
- the material to be communicated through, in this case the first author's forearm,
- a second coupling layer, and
- a second piezoelectric transducer as the receiver.

The forearm was chosen due to ease, as it is relatively thin, and made up of almost parallel facets. Also, communication through the bone structure of the forearm would be required for a device located within the chest or cranial cavities.

## THEORY

### Piezoelectric Transducer

For a complete understanding of piezoelectric materials and transducers, see Silk's *Ultrasonic Transducers for Nonde-*

*structive Testing* [10]. A brief overview is included here for completeness.

In linear elastic solids, the strain (S) and stress (T) are related by the elastic stiffness (c). In the same material, the electric displacement (D) is related to the electric field (E) by the permittivity ($\varepsilon_r$) of the material. These equations are referred to as the constitutive equations

In a piezoelectric linear elastic material, the constitutive equations are coupled. Hence, a change in stress or strain corresponds to a change in the charge distribution within the material. The constitutive equations for a piezoelectric material are [9],

$$T = cS + hE$$
$$D = \varepsilon_r E + hS, \tag{1}$$

where $h$ is the piezoelectric coupling coefficient.

## Communications

For the benefit of increased bandwidth, only digital communications methods were used for the acoustic communications. Due to the thickness of the communications medium and composite structure (bone, muscle etc), only Phase Shift Keying (PSK) was considered.

In PSK, the digital information is encoded onto the carrier wave via a phase modulation. The state of each bit of information is determined according to the state of the preceding bit. If the phase of the carrier wave does not change, then the logic level stays the same. If the phase of the carrier wave changes by 180 degrees, then the logic level changes, from zero to one, or from one to zero. Decoding PSK uses some simple mathematics to retrieve the phase information. The PSK signal;

$$f(t) = A_0 \cos(2\pi f_c t + \phi(t)), \tag{2}$$

where

$$\phi(t) = \begin{cases} 0 & \text{for } data = 0 \\ 180 & \text{for } data = 1. \end{cases} \tag{3}$$

is multiplied by a synchronous sine and cosine, giving,

$$g(t) = A_0 \cos(2\pi f_c t + \phi(t)) \times \sin(2\pi f_c t)$$
$$= \frac{A_0}{2} [\sin((4\pi f_c t + \phi(t))) + \sin(\phi(t))]. \tag{4}$$

and

$$h(t) = A_0 \cos(2\pi f_c t + \phi(t)) \times \cos(2\pi f_c t)$$
$$= \frac{A_0}{2} [\cos(\phi) + \cos((4\pi f_c t + \phi(t)))], \tag{5}$$

These two components are called the in-phase (I) and quadrature (Q) components, respectively. Both I and Q contain high and low frequency components, where the low frequency component is the sine or cosine of the time dependent phase. Using a low pass filter, the high frequency components are removed, leaving only the phase components,

$$g(t) = \frac{A_0}{2} \sin(\phi(t)). \tag{6}$$

and

$$h(t) = \frac{A_0}{2} \cos(\phi(t)), \tag{7}$$

Then by taking the arctan of I on Q, the time dependent phase information is recovered,

$$y(t) = \arctan\left(\frac{g(t)}{h(t)}\right)$$
$$= \arctan\left(\frac{\sin(\phi(t))}{\cos(\phi(t))}\right) \tag{8}$$
$$= \arctan(\tan(\phi(t)))$$
$$= \phi(t).$$

The filter used is a raised cosine filter [12]. Figure 1 shows the steps of the PSK encoding and decoding process used in the communications channel experiments. Figure 1 a) shows the digital information to be transmitted. This information is then encoded onto the square wave carrier, shown in figure 1 b), as the 180 degree phase change. This signal is then received, as shown in Figure 1 c). The phase information is then recovered, as shown in Figure 1 d), and by sampling at suitable points a phase greater than 0 is equated to a 1, and a phase less than 0 is equated to a 0.
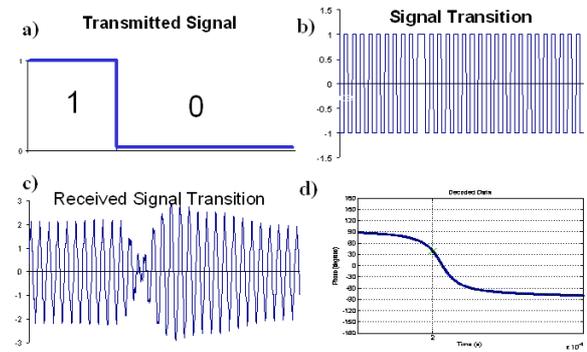


**Figure 1**. The PSK communications encoding and decoding; a) The initial digital information, b) the phase encoded signal, c) the received signal, and d) the recovered phase information

## Power Harvesting

For the power harvesting, the piezoelectric receiver is modelled as a current source, $i_p$, in parallel with with a capacitor, $C_p$. The source current can be written as [9],

$$i_P(t) = I_P \sin(\omega t), \tag{9}$$

where $I_p$ is the peak current, also refered to as the short circuit current, and $\omega$ is the angular frequency of the AC signal. The open circuit voltage, $V_{OC}$, can then be defined in terms of the short circuit current and the reactance of the capacitor ($X_C$) [11], that is,

$$V_{OC} = I_P X_C = \frac{I_P}{\omega C_P}, \tag{10}$$

To harvest power, the piezoelectric element needs to be connected across a load. In the case of the AC analysis, this is simply a load resistance. There is a 90 degree phase shift between the current flowing through the load resistor (R) and the current flowing through the capacitor. The total power can be expressed as the geometric sum of the power stored in the capacitor, and the power dissipated through the resistor. That is,

$$P_T = \sqrt{P_R^2 + P_C^2} \tag{11}$$
$$= \sqrt{I_R^2 R + I_C^2 X_C}.$$

Since the circuit is an AC current divider, the short circuit current can be expressed as,

$$I_P = \sqrt{I_R^2 + I_C^2}. \tag{12}$$

The peak power will then occur when the current flow through the capacitor and the resistor is equal. That is, the load resistance is equal to the capacitor's reactance,

$$R = \frac{1}{\omega C}. \tag{13}$$

The resistor current at peak power is then,

$$I_R = \frac{I_P}{\sqrt{2}}. \tag{14}$$

The voltage at peak power is then,

$$V = I_R X_C = \frac{I_P}{\sqrt{2}\omega C_P}. \tag{15}$$

We can also express the voltage out as a function of the resistance. From (12) we see that,

$$V = R I_P = R\sqrt{I_P^2 - I_C^2}, \tag{16}$$

The capacitor current is also a function of the voltage, so with a little algebra we see [10],

$$V = \frac{I_P R}{\sqrt{1 + (\omega C_p R)^2}}. \tag{17}$$

The power as a function of the resistance can then be expressed as,

$$P = \frac{V^2}{R} = \frac{I_P^2 R}{1 + (\omega C_p R)^2}. \tag{18}$$

## METHOD

### Acoustic Transmissions Channel Setup

The experimental setup of the acoustic-transmissions channel is shown in Figure 2. The PZT transducers used were un-backed, and coupled to the forearm using acoustic coupling gel. The piezoelectric transducers used were Steiner and Martins SMQA PZTs. They had a thickness of 2.1mm, corresponding to a resonant frequency of 1MHz, and a radius of 10mm.

### Acoustic Communications

Testing the communications involved looking at a number of different quantities. These included,
- the transfer function,
- the frequency response,
- the transient response, and,
- the data rate.

First, the transfer function of the communications channel was measured. The function generator was set to give a continuous sine wave at the resonant frequency of the PZT trans-

ducers, 1MHz. The amplitude was then varied from 1 volt to 10 volts. Values were recorded at 1 volt increments. This process was repeated several time to give an average and statistical uncertainty.
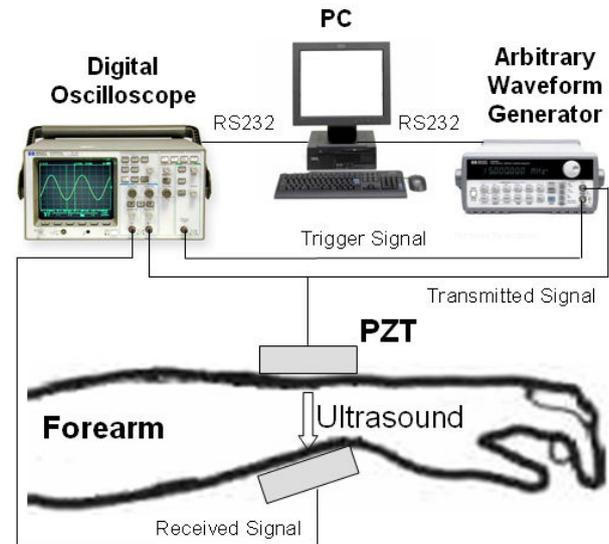


**Figure 2**. The setup of the acoustic-transmissions channel

Next, the frequency responses of the communications channel were determined. The function generator was set to give a continuous sine wave at maximum voltage, 10 Volts peak. The frequency was then varied from 10 kilohertz to 2 Megahertz. Values were recorded every 10 kilohertz.

Finally, the transient response of the communications channel was investigated, using a low rate sine wave burst at 1MHz with 100 cycles. The trailing signal is also examined to determine if it will have any adverse effects on the performance of the communications channel.

The communications signals were generating on an Agilent 33120A arbitrary waveform generator. ASK (specifically OOK) signals were generated using the burst function of the generator. A 1MHz sine wave carrier was used with a data rate of 40kbps. The PSK signals were generated in the Waveform Editor software for the waveform generator. The signals were then flashed to the device via the computer interface. The waveform generated consisted of a sine wave carrier, with a data rate of 1/100 the carrier frequency (the software does not generate time so the frequency is set and varied on the generator, and hence a ratio is used). So for the carrier wave frequency of 1MHz, the data rate was 10kbps.

All of the communications signals were recorded on the digital oscilloscope, and downloaded to a PC. The demodulation of the signals was then implemented in Matlab[TM] [13].

### Power Harvesting

For the preliminary acoustic power harvesting, the AC performance was analysed. In the AC circuit experiments, first the capacitance of the piezoelectric element was measured using a capacitance meter. After calculating the reactance at the resonant frequency, the output of the piezoelectric receiver was applied to a variety of suitable load resistors. The voltage drop across the load resistor was measured using a 1MΩ Digital Storage Oscilloscope (DSO). To compare the experimental results to the theoretical analysis, the AC circuit was also simulated in PSpice. The value of $I_p$ was obtained using (10), with the measured values of $C_p$ and $V_{OC}$. A parametric analysis was performed, varying the value of the load resistance in a frequency domain analysis. The load value

was swepted from 10Ω to the value of the DSO, 1MΩ at 10 points per decade. Figure 3 shows the circuit diagram for the power harvesting simulations. For the experiments, this simply required the load resistance to be placed between the received line and ground of Figure 2.
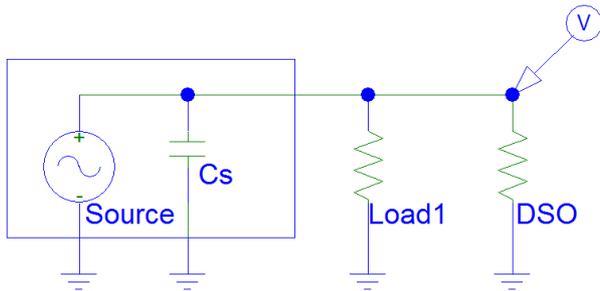


**Figure 3**. The PSpice simulation circuit, with the AC current source and the source capacitor as the piezoelectric receiver in parallel with the Load and DSO

## RESULTS

### Transfer Function

Figure 4 shows the transfer function of the acoustic-communications channel at 1MHz. The relationship between the input signal strength and the output signal strength is linear, with a coefficient of 1, which corresponds to a 100% efficiency. The noise in the curve is due to small movements in the transmission medium.
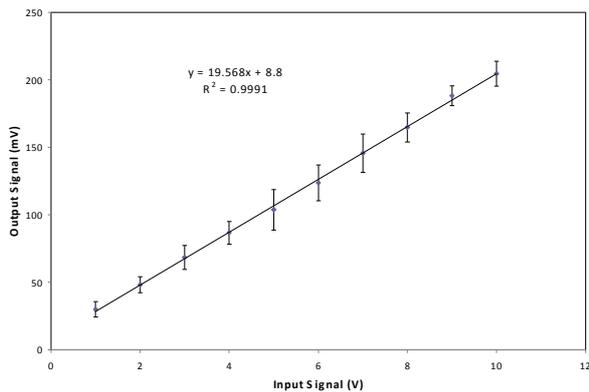


**Figure 4**. The transfer function of the acoustic communications channel at resonance

### Frequency Response

The frequency response of the acoustic-communications channel is show in figure 5. As expected, a strong peak in the frequency spectrum occurs at the resonant frequency of the piezoelectric transducers, that is, 1MHz. A secondary peak is noticeable at 100kHz.
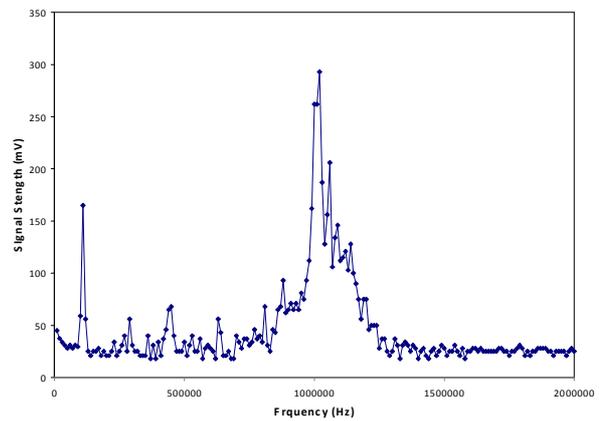
### Transient Response

Figure 6 show the transient response of the acoustic-communications channel for 100 cycles at 1MHz. The compact burst has a minor tail effect, elongating in time. One of the main reasons for this is due to the composite nature of the communications channel. The various materials which the body is made up of all have different acoustic velocities. The result of this is that the various paths travelled by the ultrasound in the medium will result in significant temporal dispersion, and then interference. Figure 7 show the transient response with enough cycles to achieve steady-state. The rise time is then given by approximately 25 cycles, at 1MHz, giving 25μs.



**Figure 5**. The frequency response of the acoustic communications channel
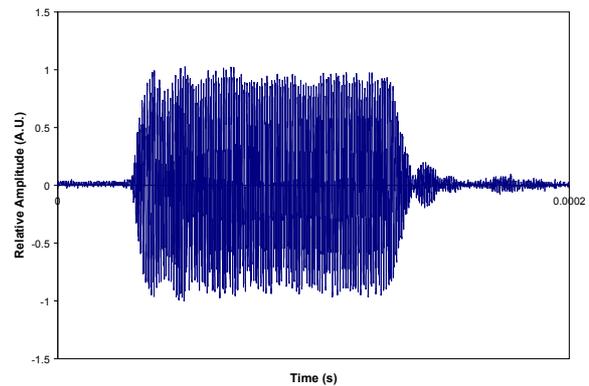


**Figure 6**. The transient response of the acoustic communications channel to an input tone burst
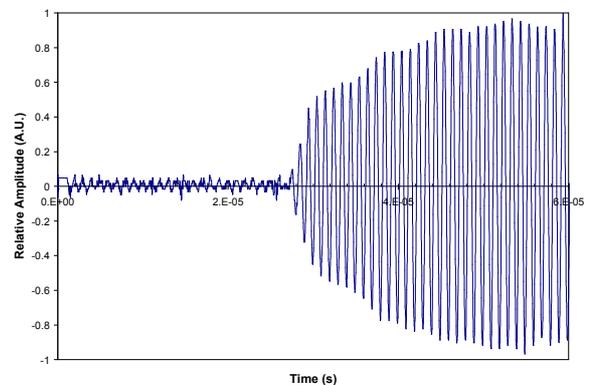


**Figure 7**. The transient response of the acoustic communications channel showing the rise time

### Acoustic Communication

The results of the acoustic communications test are shown in Figures 8 to 11. Figure 8 shows the transmitted ASK (OOK) signal. Ringing is noticeable as the signal is switched off. Figure 9 shows the received ASK (OOK) signal. A low pass filter at above the data rate, but below the carrier frequency, will recover the envelope, and the use of a comparator with a suitable compare level will enable the digital information to be recovered.

Figure 10 shows the received PSK signal, which contains the data stream [1 1 0 0 1 0 1 1 1 1]. The decoded PSK signal is then shown in Figure 11. The original digital information can be recovered by selecting a digital 1 as a phase less than 0 degrees, and a digital 0 as a phase greater than 0 degrees.

Note that the transmitted PSK signal is not shown, as no information is visible on the time scale of the entire signal.
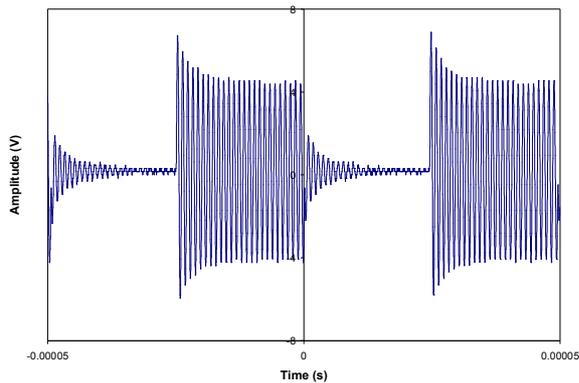


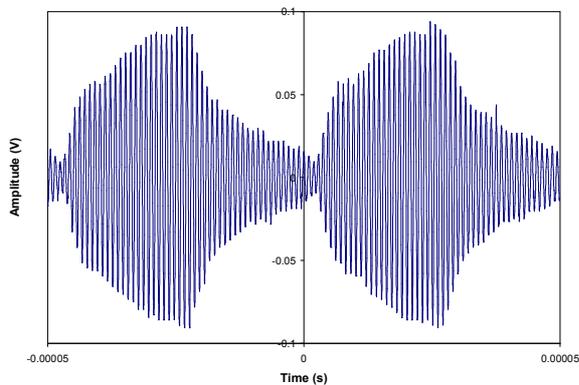**Figure 8**. The transmitted ASK (OOK) acoustic communications signal



**Figure 9**. The received ASK (OOK) acoustic communications signal
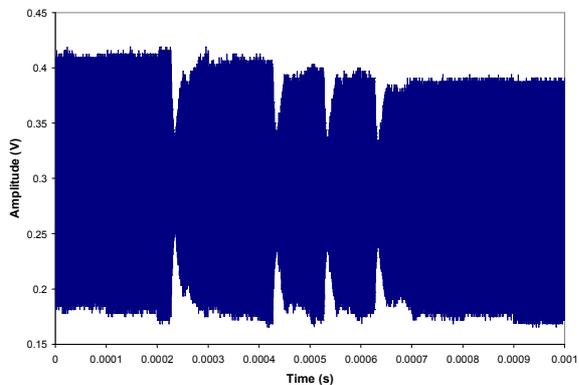


**Figure 10**. The received PSK acoustic communications signal

## Power Harvesting

The capacitance of the piezoelectric receiver was measured to be 1.086nF. At the resonant frequency of 1.035MHz, this gives a reactance of 141Ω. With an open circuit voltage of 570mV, (10) gives a short circuit current of 4mA. These values where then used in the PSpice simulation of the AC circuit.

Figure 12 shows the comparison between the applied load and the voltage drop across it, for both the experimental values and the simulated results. As expected, as the load resistance decreases in size, the output voltage also decreases.

Figure 13 shows the load current as a function of the output voltage (IV curve), and Figure 14 shows the power delivered to the load as a function of the output voltage (PV curves), for the experimental, theoretical and simulated results. The PV curve shows a measured peak power of 1mW, while theory and simulation give peak power values of 1.121mW and 1.125mW, respectively.
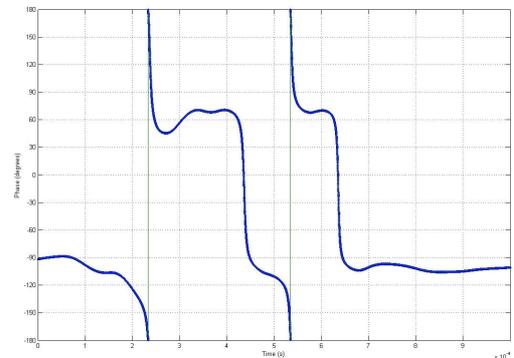


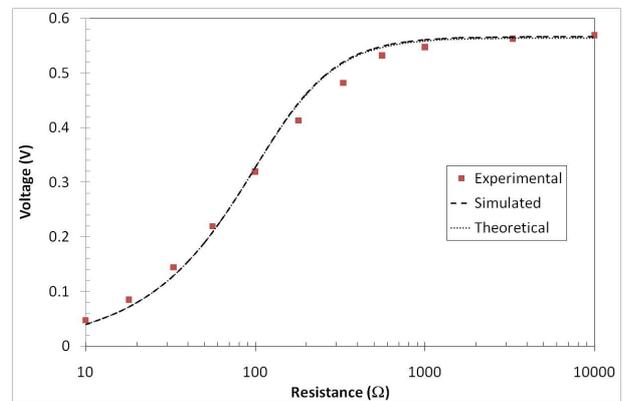**Figure 11**. The decoded PSK acoustic communications signal [1 1 0 0 1 0 1 1 1 1]



**Figure 12**. Voltage as a function of load resistance for the power harvesting
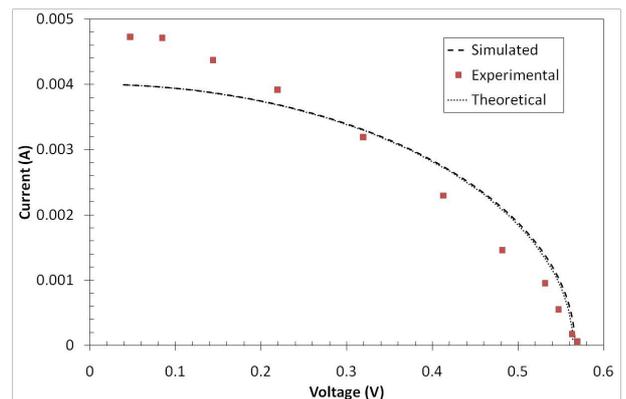


**Figure 13**. Load current as a function of the voltage, IV curve

## DISCUSSION

As expected, the transfer function is linear. Some randomness is noticeable in the signal, hence the uncertainty. It is worth noting that a similar uncertainty would be expected on all other results. The experiments were preformed with the arm as immobile as possible. A significant variation was noticed when the arm/hand was allowed to articulate. The peak value varied from around 140mV to 280mV, a factor of 2. This fluctuation may be an issue, in particular if ASK is used as

the encoding method. It is for this reason that PSK would be a far more robust encoding method.
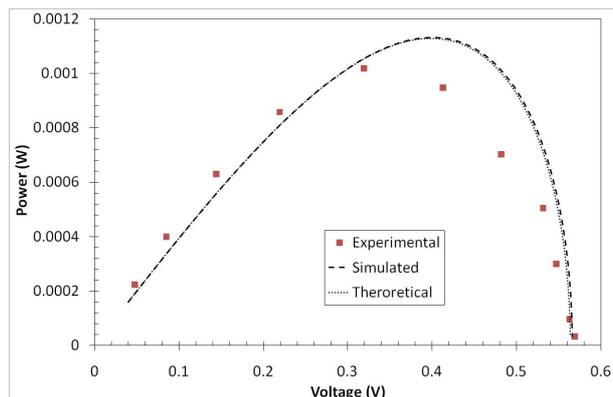


**Figure 14**. Power delivered to the load as a function of the voltage, PV curve

The result of the transient response suggests that relatively high data rates may be achievable, specifically if a transducer with a higher resonant frequency was to be utilised. The use of a high communications rate would reduce the effect of fluctuations due to motion of the communications medium. The ASK communications signal show the relatively high data rate that may be achievable; that is, a data rate of 40kbps with a 1MHz carrier frequency. The result of the PSK communications signal, figure 10, also shows that a relatively high data rate is possible. The phase transitions are not as quick as those show in previous work [6], when communicating through an aluminium panel, but the data rate is relatively high for the intended application.

The preliminary results for the power harvesting are promising. The value of 1mW was significant compared to values expected. However, in the attempt to implement an AC to DC converter, the very high frequency appears to be limiting the ability to successfully rectify the output of the transducer. This is mainly due to the high junction capacitance of the rectifier diodes. In the conversion from AC to DC, the capacitance is an important consideration to achieve peak power output [9]. To resolve this issue, we intend to aquire transducers with a lower resonant frequency, in the kiloHertz range, and quantify the performance of the power conversion as a function of frequency.

However, with the successful implementation of an AC to DC converter, the measured power levels could easily be utilised for the in-vivo recharging of a device such as a pacamaker [14].

## CONCLUSION

In conclusion, we have successfully used acoustic transmissions to both communicate and harvest power through a biological medium, in-vivo. The acoustic communications show great promise for utilisation in practical communications with in-vivo biomedical devices; specifically in those applications where local heating effects of wireless RF transmission is prohibitive. Even if the data rate was lowered in order to reduce the bit error rate, and increase reliability, a significant data rate could be utilised, more than is necessary for static biomedical devices. The power that can be delivered through the channel is also promising, especially for low power devices, such as pacemakers and neural implants.

## REFERENCES

1   V. K. Varadan, "The role of nanotechnology and nano and micro-electronics in monitoring and control of Cardiovascular diseases and neurological disorders," Proc. SPIE **6528** (2007)

2   C. Kim, T. Lehmanna and S. Nooshabadib, "An ultra-wideband transceiver for biotelemetry systems," Proc. SPIE **6798** (2007)

3   C. Gabriel, S. Gabriely and E. Corthout, "The dielectric properties of biological tissues: I. Literature survey," Phys. Med. Biol. **41**, 2231–2249 (1996)

4   S. Gabriely, R.W. Lau and C. Gabriel, "The dielectric properties of biological tissues: II. Measurements in the frequency range 10 Hz to 20 GHz," Phys. Med. Biol. **41**, 2251–2269 (1996)

5   S. Gabriely, R.W. Lau and C. Gabriel, "The dielectric properties of biological tissues: III. Parametric models for the dielectric spectrum of tissues," Phys. Med. Biol. **41**, 2271–2293 (1996)

6   G. Wild, "Design and evaluation of an electro-acoustic communications channel for use by autonomous agents in the structural health monitoring of ageless aerospace vehicles," Honours Thesis (Edith Cowan University, 2005)

7   G. Wild and S. Hinckley, "Electro-acoustic and acousto-optic communications for robotic agents in smart structures," Proc. SPIE **6414** (2006)

8   G. Wild and S. Hinckley, "Wireless acoustic communications for autonomous agents in structural health monitoring sensor networks," Proc. SPIE **6798** (2007)

9   G.K. Ottman, et al., "Adaptive piezoelectric energy harvesting circuit for wireless remote power supply" IEEE Trans. Power Electron. **17**(5), 669-676 (2002)

10  M.G. Silk, *Ultrasonic Transducers for Nondestructive Testing* (Adam Hilger Ltd, Bristol, 1984).

11  M. Guan and W.H. Liao, "Comparative analysis of piezoelectric power harvesting circuits for rechargeable batteries" in *Proceedings of the 2005 IEEE International Conference on Information Acquisition* (IEEE, 2005) pp. 243-246

12  J. Proakis and M. Salehi, *Communication Systems Engineering* (Prentice Hall, New Jersey, 1994)

13  Mathworks Inc.

14  V.S. Mallela, V. Ilankumaran and N.S. Rao, "Trends in cardiac pacemaker batteries" Indian Pacing Electrophysiol. J. **4**(4), 201–212 (2004)